Microstructures and fracture behavior of glass-fiber reinforced PBT/PC/E-GMA elastomer blends—1: microstructures

Ke Wang[a,b], Jingshen Wu[a,*], Hanmin Zeng[b]

[a]*Department of Mechanical Engineering, The Hong Kong University of Science and Technology, Clear Water Bay, Kowloon, Hong Kong SAR, China*
[b]*Institute of Materials Science, Zhongshan University, Guangzhou, China*

Abstract

A group of glass-fiber-reinforced polymer composites with controlled morphology were designed and prepared by sequential compounding of poly(butylene terephthalate)/glass-fiber (PBT/GF) composite with a reactive elastomer, ethylene-co-glycidyl methacrylate (E-GMA), and/or polycarbonate (PC). The microstructures of the composites were characterized by means of AFM, SEM and thermal analysis. The results indicate that the glass fiber was surrounded by a dead layer of PBT. In the matrix, the E-GMA particles, of sizes varying between 0.5 and 1 μm, were encapsulated by the PBT phase. The PBT and PC formed an interconnected phase structure with a PBT domain thickness of about 1 μm and the PC domain thickness of less than 0.5 μm. It was found that when the PBT/GF was mixed with the E-GMA in the first step of the sequential blending, the epoxide groups in the E-GMA tended to homo-polymerize through ring-opening rather than to react with the carboxyl and/or hydroxyl groups of the PBT. Consequently, a slightly cross-linked structure formed in the E-GMA phase, which kept the E-GMA domains to stay in the PBT phase during the second step of the sequential blending with the PC. On the other hand, the transesterification between the PBT and the PC resulted in a decrease in the PBT chain regularity, leading to a lower crystallization rate and formation of crystallites with low perfection. © 2001 Elsevier Science Ltd. All rights reserved.

Keywords: Poly(butylene terephthalate); Polycarbonate; E-GMA copolymer; Glass fiber; Microstructures

1. Introduction

Recently, rigid-polymer-toughened polymer blends (rigid-rigid polymer blends) have attracted considerable attention [1–4]. Unlike rubber-toughened polymers, the toughness of the rigid-rigid polymer blends can be improved without sacrificing too much of the other properties, such as stiffness, strength, creep resistance and heat distortion temperature, etc.

Poly(butylene terephthalate) (PBT) is one of the most important engineering polymers with a wide range of applications because it possesses good tensile strength, flexural modulus, dimensional stability and high resistance to hydrocarbons. However, PBT has relatively low impact strength and much research effort has been put into improving its toughness. Of the resulting products, the PBT/PC blend is one of the most widely used PBT based blends and the structure-property relationships of PBT/PC blends have been studied extensively [5–16].

In a series of studies [10–13], Wu and co-workers reported a synergistic effect in PBT/PC blends containing 40 to 50% PBT. The quasi-static fracture toughness of these blends was much higher than that of the pure components. At the same time, both the modulus and the yield stress showed positive deviation from the rule of mixtures. Accordingly, it was found that the interfacial adhesion in these blends was relatively stronger than that of blends containing more than 60% PBT which showed poor mechanical properties. It was then proposed [12] that the copolyester formed during melt blending enhanced the interfacial bonding between the PBT and PC domains, which, in turn, resulted in the significant improvement of the mechanical properties of the PBT/PC blends.

Given the importance of the copolyester in the toughening of the PBT/PC blends, the effect of the interfacial adhesion strength on the properties of the PBT/PC blends was studied in a following work [14] by incorporating different amounts of the PBT-PC copolyester into the PBT/PC blends. It was revealed that addition of

---

the PBT-PC copolyester could improve the compatibility between the PBT and PC, which resulted in enhanced interfacial adhesion and decreased domain size. The improved interfacial bonding and decreased domain size rendered the blends with a higher value of the specific essential fracture work.

On the other hand, it was found that [13,14] the impact toughness of the PBT/PC blends was low. Failure mechanism studies disclosed that the PBT is a strain rate sensitive polymer. It becomes more rigid at higher strain rate and imparts a high plastic constraint on the ductile PC domains. The high plastic constraint will maintain plane-strain conditions at the crack-tip and promote brittle fracture for the blends, leading to low impact toughness.

From the material design point of view, it was proposed that [13], if the strain rate sensitivity of the PBT can be reduced, the impact toughness of the PBT/PC blends may be improved. To confirm the propositions, we attempted to reduce the strain rate sensitivity of the PBT by introducing a small amount of elastomer into the PBT phase of a PBT/PC blend via sequential blending. To compensate for the yield strength and modulus loss due to the elastomer addition, short glass fibers were used as reinforcements. Mechanical testing results of the GF reinforced PBT/PC/elastomer composites show that the composites have a significantly improved impact strength, which stems from the unique microstructures of the composites formed during the sequential blending. In the present paper, the morphology of the designed composites is disclosed. The mechanical properties and toughening mechanisms of the composites will be reported in the second part of this series.

2. Experimental

2.1. Materials

Two kinds of commercial PBT resin were used in the present study. One was a PBT homopolymer (Toray 1401, Japan) and the other was a PBT/GF composite (Toray 1101G-30, Japan) containing 30% glass fiber. The PC (Calibre 201) was supplied by Dow Chemical Co. with a melt flow rate of 15 g/10 min. The impact modifier (IM) (IGETABOND BF/7M) is an ethylene-co-glycidyl methacrylate (E-GMA) copolymer containing 12% GMA, which was purchased from Sumitomo Chemical Co.

2.2. Compounding and injection molding

Based on our previous study on the PBT, PC and elastomer system [10–13], we believe that it is beneficial for toughness enhancement to locate the rubbery phase in the PBT rather than in the PC, as the strain rate sensitivity of the PBT will be reduced. Since a simple simultaneous mixing of PBT, PC and E-GMA in an extruder may not produce the required blends with the E-GMA in the PBT phase, a sequential blending process, during which the PBT and E-GMA would be mixed thoroughly before addition of PC, was designed and employed in the present work. The details of the sequential blending process are described as follows.

Before compounding, the PBT and PC pellets were dried at 120 °C for 5 h in an air-circulating oven. In the preparation of the (PBT/GF)/IM and (PBT/GF)/PC composites, the dried pellets of PBT/GF and IM, or PC, were first mixed manually and then compounded in a twin-screw extruder (ZSK-30, L/D = 29/1) at the temperatures and screw speeds shown in Table 1. The resident time of the components inside the extruder was approximately 4 min, which was measured by adding pellets of different colors. The resultant (PBT/GF)/IM, or (PBT/GF)/PC, composites were pelletized and dried at 120 °C for 5 h before they were injection molded into testing samples.

In the preparation of the (PBT/GF)/IM/PC composite, the IM and PBT/GF were mixed in the extruder for about 11–12 min before addition of PC to ensure the IM elastomer to disperse in the PBT phase. This prolonged mixing time was achieved by three consecutive extrusions of the (PBT/GF) and IM. In the first extrusion, the dried PBT/GF and IM pellets were compounded under the conditions listed in Table 1. The resultant (PBT/GF)/IM composite was pelletized, dried and then extruded for the second time under the same condition. The re-extruded (PBT/GF)/IM composite was pelletized, dried and re-extruded again for the third time. After three consecutive extrusions, the accumulated compounding time for the (PBT/GF)/IM composite was about 11–12 min. The resultant (PBT/GF)/IM composite was then melt mixed with PC. The procedure is schematically shown as follows:
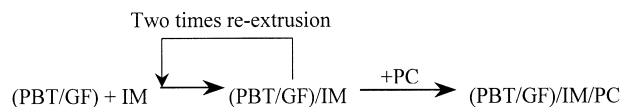
The content of glass fiber was kept at 16 wt.% in all the samples and the compositions of the composites are listed in Table 1. Rectangular bars (125×12.7×3 mm) were injection molded at 250 °C. The mold temperature was kept at 50 °C.

2.3. Morphology observation

Several attempts were made to discover the morphological details of the matrix of the composites. Atomic force microscope (AFM) and scanning electron microscope (SEM) were employed using the samples prepared by different methods.

The AFM analyses were performed on a DI TAX 2000 AFM under ambient conditions in the tapping mode.

Table 1
Compositions and processing conditions of the blends

Material Code	PBT (%)	PC (%)	IM (%)	GF (%)	Processing temperatures (°C)				DIE	Screw speed (rpm)	Resident time (min)
					Zone 1	Zone 2	Zone 3	Zone 4			
(PBT/GF)/IM	74		10	16	240	250	250	250	240	25–30	∼4
(PBT/GF)/PC	44	40		16	240	250	250	250	240	25–30	∼4
(PBT/GF)/IM/PC	38	36	10	16	240	250	250	250	240	25–30	11–12

Phase images were acquired using the 512×512 pixels at a scan rate of 0.3 Hz. The AFM samples were prepared according to the following procedure. Blocks cut from the injection molded rectangular bars were embedded in an optically clear epoxy. After curing at room temperature for 24 h, one end of the epoxy cylinder was cut with a diamond saw to reveal the middle section of the sample block with the cutting plane perpendicular to the melt flow direction (MFD). The fresh cut surface of the cylinder was then polished with different grade diamond paste (6, 3 and 1 μm) and an aluminum oxide powder (0.3 μm) until it was completely suitable for AFM observation.

The samples for SEM observation were first annealed at 80 °C for 10 h to ensure sufficiently high degree of crystallization of the PBT phase. Then, the annealed samples were embedded, cut, and polished following the same procedure of preparing the AFM samples. Afterwards, two etching methods were used to selectively remove one or two components from the matrix in order to reveal the microstructure of the matrix. In the first method, the polished surfaces were etched with boiling dichloromethane for 30 min. Since PBT is insoluble in dichloromethane, the IM and/or the PC phase will be extracted. The second method is dipping the samples in a solution of 1% potassium hydroxide (KOH) in methanol at room temperature for 20 min to hydrolyze the PC phase. The etched surfaces were then washed, dried and coated with a 150 Å-thick gold layer and observed with a Jeol 6300 SEM.

2.4. Thermal analysis

DSC measurements were conducted using a Setaram DSC92 DSC apparatus. The samples (∼20 mg) were first kept at −50 °C for 5 min and then heated to 300 °C at a heating rate of 10 °C/min. After being annealed at 300 °C for 5 min, the samples were cooled down to −50 °C at a cooling rate of 10 °C/min and kept at −50 °C for 5 min. Afterwards, the samples were reheated to 300 °C at a heating rate of 10 °C/min. The glass transition temperature (T_g) was determined and the peak temperature of the exotherm and endotherm in the thermograms were taken as the crystallization temperature (T_c) and melting temperature (T_m), respectively. The degree of crystallinity of the PBT component was obtained using a value of 142 J/g for perfect PBT crystals.

3. Results and discussion

3.1. AFM observations

The AFM phase images of the composite samples are shown in Fig. 1a–c. Different domains can be distinguished by the shades of the images. As tapping mode was used, a brighter region, thus, represents a harder domain, and vice versa. Fig. 1a is the AFM phase image of the (PBT/GF)/IM, the brightest quarter-sphere region
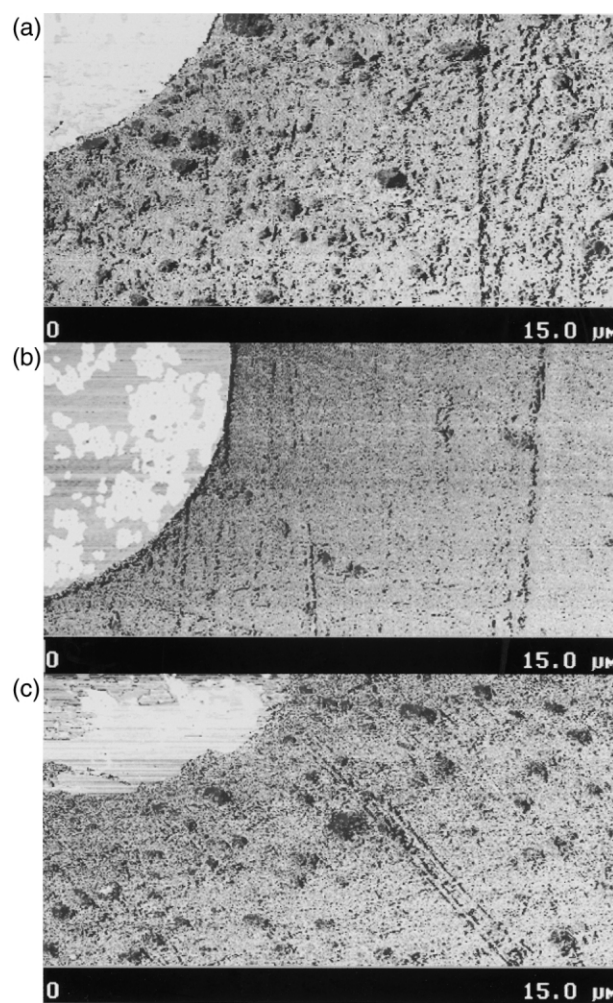

Fig. 1. AFM phase images of (a) (PBT/GF)/IM; (b) (PBT/GF)/PC; (c) (PBT/GF)/IM/PC.

at the upper-left corner is corresponding to the cross section of the glass fiber. The glass fiber is surrounded by the PBT matrix with dispersed IM domains (the darkest dots). The shape of the IM particles in the (PBT/GF)/IM is irregular with domain size of 0.5–1 μm. Unlike the (PBT/GF)/IM, the matrix microstructure of the (PBT/GF)/PC composite is undistinguishable under AFM. As shown in Fig. 1b, only two phases, i.e. a glass fiber and a seemingly homogeneous matrix, can be seen. It is known that PBT and PC have similar rigidity, thus the AFM cannot detect the difference between the two components by tapping. For the same reason, there are only two phases can be seen in the matrix of the (PBT/GF)/IM/PC (Fig. 1c). Clearly, the IM particles in the (PBT/GF)/IM/PC have similar shape and particle size as in the (PBT/GF)/IM. It seems that the existence of the PC phase has no significant influence on the dispersion of the IM phase. On the other hand, we found that it is impossible to define the location of the IM domains, i.e. whether the IM domains are in the PC phase or in the PBT phase, by AFM.

Additionally, it is noted in Fig. 1a and c that the number of the IM particles neighboring the glass fiber is higher than that far away from the glass fiber, which was found to be an important morphological factor influencing the fracture behavior of the composites. The details on this issue will be discussed in the second part of this series [16].

3.2. SEM observation

3.2.1. Dichloromethane etched samples
To disclose the microstructures of the composite matrix, the polished sample surfaces were etched using dichloromethane. As expected, the PBT was stable in dichloromethane so that the surface of the (PBT/GF) sample remained smooth after the chemical extraction (Fig. 2). In the (PBT/GF)/IM case (see Fig. 3), the IM
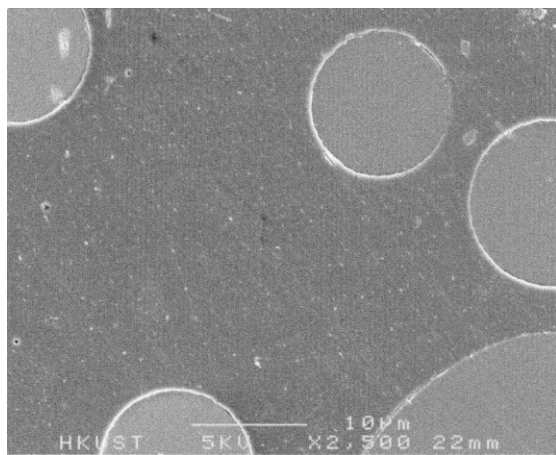
phase was extracted out of the matrix and a number of small holes of 0.5–1 μm in diameter were left on the sample surface. This result is in good agreement with the AFM observations.

With removal of the PC phase from the matrix, the microstructure of the (PBT/GF)/PC composite was revealed. As can be seen in Fig. 4a and b, the PBT/PC blend matrix has a very fine, interconnected morphology. The details of the phase structure can only be distinguished under high magnification. It is estimated from Fig. 4c that the thickness of the PBT domain is about 1 μm or slightly larger, which is in the same order as the IM particles. The PC domain seems much finer; the thickness is less than 0.5 μm.

The morphology of the (PBT/GF)/IM/PC composite shown in Fig. 5a and b exhibits a combined characters of the (PBT/GF)/IM and the (PBT/GF)/PC. Holes corresponding to the extracted IM domains with diameter from 0.5 to 1 μm disperse randomly on the etched surface with fine PBT/PC textures. Once again, the IM particle number in the area near the fibers is found to be larger than that in the area far away from the fibers. However, it is still difficult to make a conclusion with confidence on the location of the IM particles, although
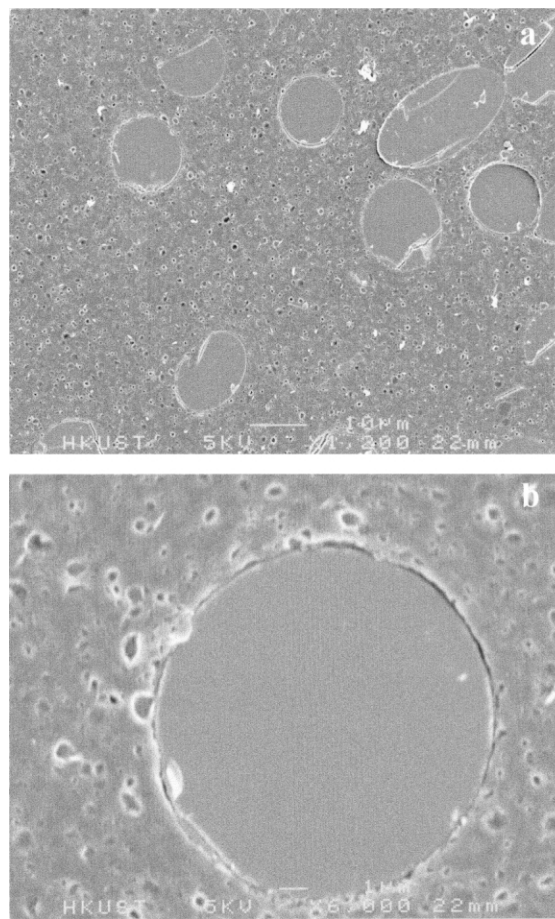

Fig. 3. SEM micrographs of the chloromethane etched surface of the (PBT/GF)/IM: (a) ×1200; (b) ×6000.

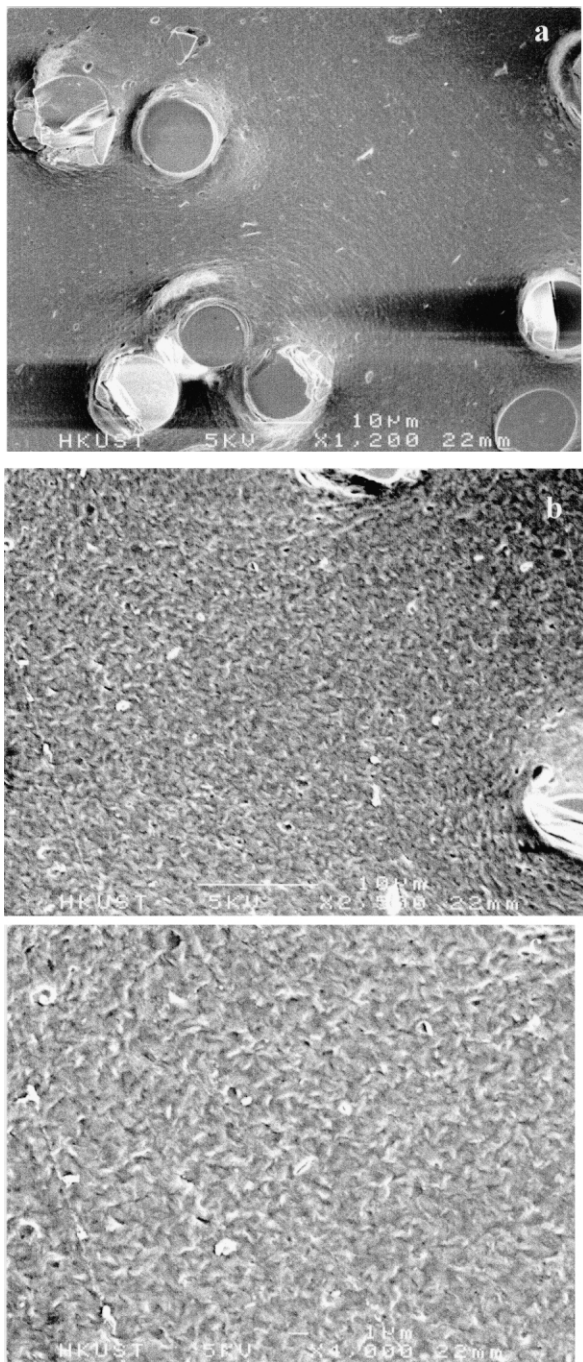Fig. 2. SEM micrographs of the chloromethane etched surface of the (PBT/GF)×2500.

Fig. 4. SEM micrographs of the chloromethane etched surface of the (PBT/GF)/PC: (a) ×1200; (b) ×2500; (c) ×4000.

Fig. 5. SEM micrographs of the chloromethane etched surface of the (PBT/GF)/IM/PC: (a) ×1500; (b) ×2500.

it is obvious that the domain size of the PC is probably too small to host the IM particles.

On the other hand, a common feature of the (PBT/GF)/PC and the (PBT/GF)/IM/PC is that the top layer of the matrix material has been removed by the chemical and the glass fibers protrude from the etched surfaces, as can be seen in Figs. 4a and 5a. Evidently, this is caused by the fact that the PBT and the PC had formed an interconnect structure. When the PC was dissolved in
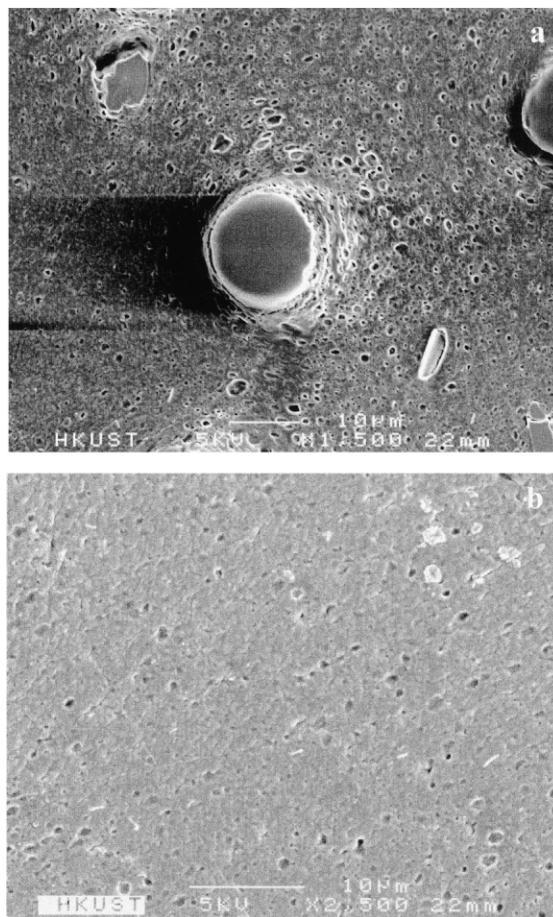
the dichloromethane, the PBT domains next to the PC phase would lose connections and fall off from the sample surface as insoluble particles.

It is also noted that a layer of matrix remained on the glass fiber after etching, forming a "sheath" on the fiber surface. As this layer is relatively stable in dichloromethane, it must be a PBT-rich phase. It is believed that such a PBT-rich sheath may be related to the pretreatment of the glass fiber during the manufacture of the PBT/GF composites. The existence of such a sheath is confirmed by the SEM examination on the fracture surface of the composites. As can be seen in Fig. 6, the "sheath" is found on the glass fibers of all four composites. Nevertheless, the thickness of this sheath varies with the composition of the composites. It is about 0.2 µm in the (PBT/GF) and the (PBT/GF)/PC and, approximately 0.5 µm in the (PBT/GF)/IM. Interestingly, a very thick sheath with a thickness of about 5 µm is observed in the (PBT/GF)/IM/PC composite. The surface of this sheath suggests significant plastic deformation of the matrix. This microstructure has a critical effect on the micro-deformation mechanisms and toughness of the composite, as will be discussed in a coming paper [16].
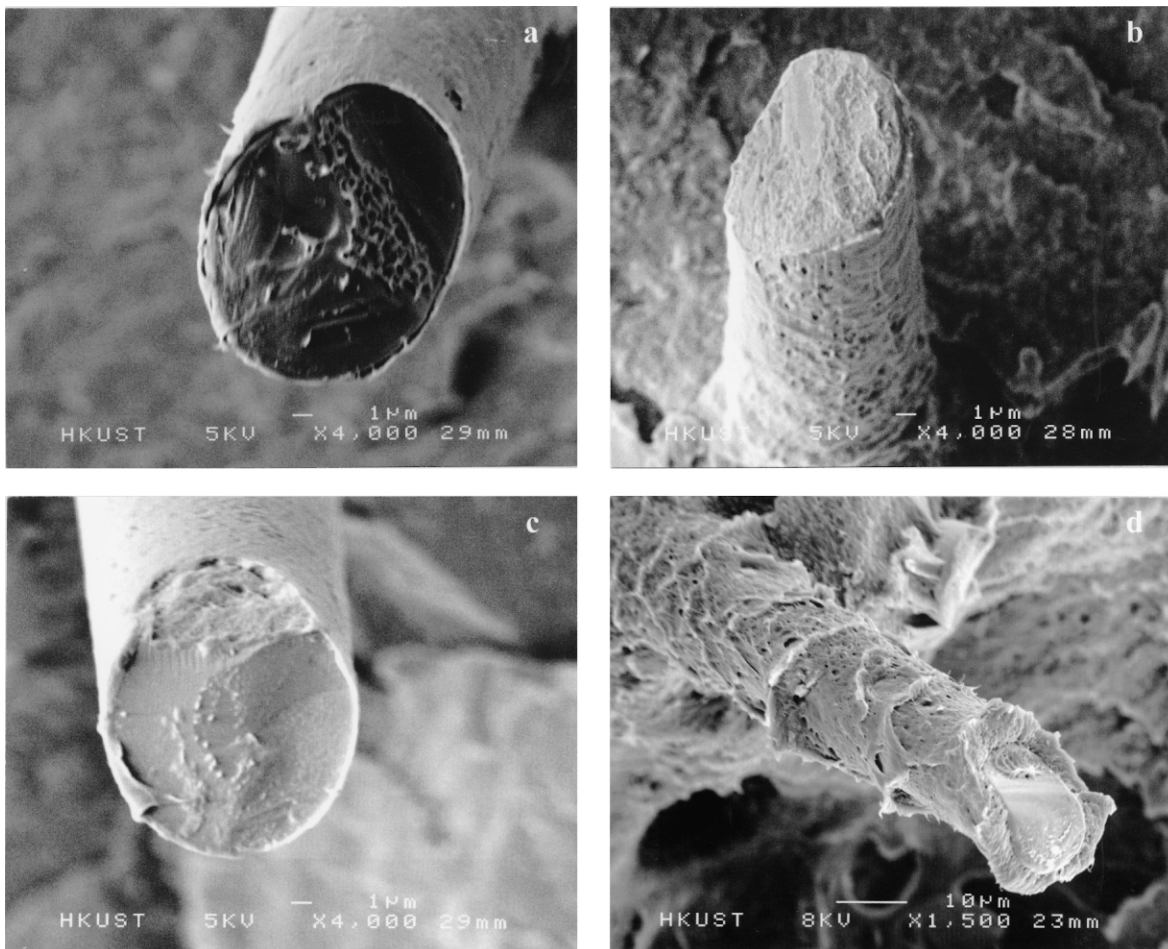
Fig. 6. SEM micrographs of the fracture surface of the composites, showing the "sheath" on the glass fibers: (a) (PBT/GF); (b) (PBT/GF)/IM; (c) (PBT/GF)/PC; (d) (PBT/GF)/IM/PC.

3.2.2. KOH solution etched samples

To identify the location of the IM domains in the (PBT/GF)/IM/PC, another set of samples were etched with KOH solution and observed with SEM. Among the components involved in the current work, the PC is the only material that can be removed by the KOH etching. If the IM domain was encapsulated in the PC phase, some IM particles would appear on the etched surface after a layer of PC had been extracted. The KOH etched surface of the (PBT/GF)/IM/PC would have a number of bulgy particles displaced randomly on a fine texture background. On the other hand, if the IM domains were encapsulated in the PBT phase, no trace of the IM phase would be found at the KOH-etched surface.

The experimental results are shown in Figs. 7–10. As expected, the surfaces of the (PBT/GF) and the (PBT/GF)/IM keep unchanged (Figs. 7 and 8), whereas the KOH-etched surface of the (PBT/GF)/PC (Fig. 9) shows a two-phase structure similar to that etched with dichloromethane. The bulgy ridges, corresponding to the PBT domains, are separated by the gullies, corresponding to the PC domains.
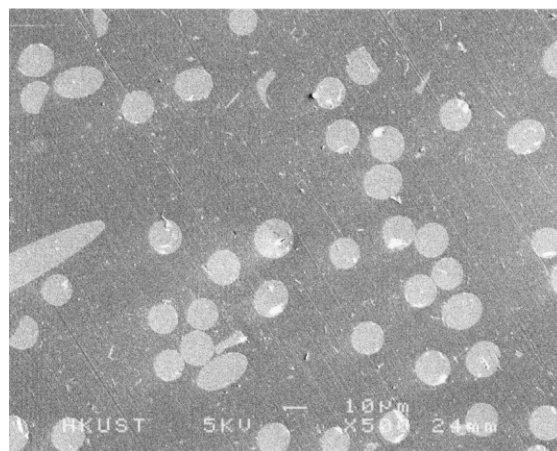

Fig. 7. SEM micrographs of the KOH etched surface of the (PBT/GF), ×500.

The pattern of the KOH-etched (PBT/GF)/IM/PC (Fig. 10) is similar to that of the (PBT/GF)/PC except that the domain size is smaller. These results are consistent with that obtained with the dichloromethane-etched samples. There are only a few large particles, as
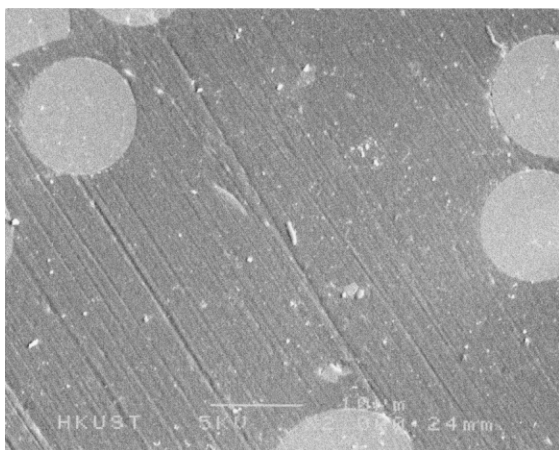
Fig. 8. SEM micrographs of the KOH etched surface of the (PBT/GF)/IM, ×2000.

indicated by arrows, can be seen on the etched surface. Evidently, most of the IM domains have been encapsulated in the PBT phase and cannot be observed, as we had expected from the sequential blending process.

3.3. Miscibility and phase structure

The AFM and SEM observations show that, in the (PBT/GF)/IM/PC composite, the PBT and PC have formed an interconnected phase structure with the PBT domain thickness of about 1 μm and PC domain thickness of less than 0.5 μm. The IM domain preferably dispersed in the PBT domains. We believe that the formation of such morphology is the results of sequential blending and the reactions between the components, as discussed below.

3.3.1. PBT/PC

The blend system of PBT and PC has been studied by many researchers [17–21] and different results about the miscibility of this polymer pair can be found in literature. Most published results [17–21] suggest partial miscibility of the components in melt blend, and the miscibility is often attributed to the exchange reactions between PBT and PC. It has been demonstrated [21] that the transesterification is the most important exchange reactions and results in the formation of random PBT-PC copolyesters, which can improve the miscibility between the PBT and the PC, leading to a fine phase structure [18,19].

Apart from the microscopic observations, the DSC analysis can also provide valuable information about the miscibility. The general features of miscible blends are the closing up of the glass transitions of amorphous domains and the depression of crystallization. In the present study, the obtained thermograms are shown in Figs. 11–13. Data including melt temperature (T_m), crystallization temperature (T_c), glass transition temperature (T_g) and crystallinity were acquired and listed in Table 2.
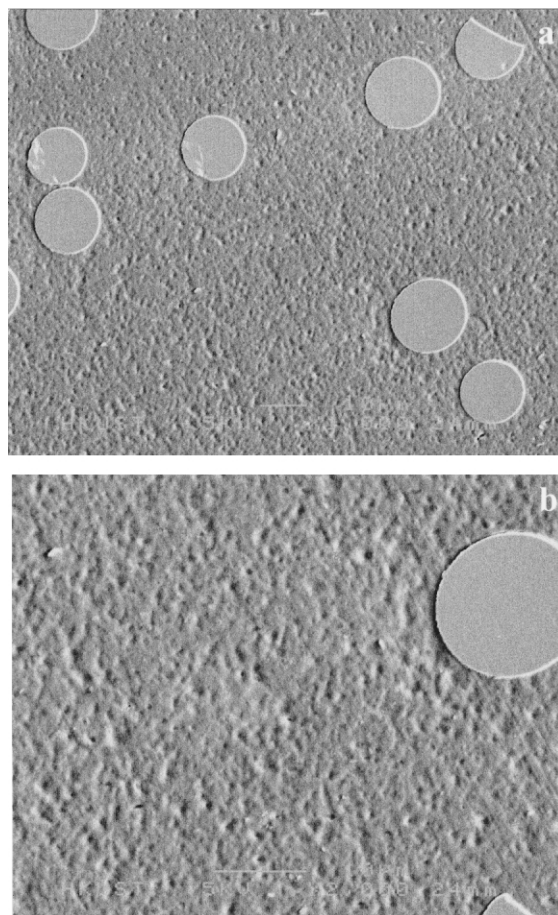

Fig. 9. SEM micrographs of the KOH etched surface of the (PBT/GF)/PC: (a) ×1000; (b) ×2000.

Fig. 11 shows the thermogram of the as-received samples in the first heating scan. It can be seen that the PBT in the (PBT/GF) composites melts at about 225 °C and shows no cold crystallization exotherm on heating, meaning that the crystallization rate of the PBT was high and the crystallization process had completed during the cooling process before the first heating. When the PC was incorporated into the PBT, i.e. in the (PBT/GF)/PC and (PBT/GF)/IM/PC cases, the melt endotherm of the PBT shifted to lower temperatures, and a cold crystalline exotherm appears at about 96 °C. In the subsequent cooling scan (Fig. 12), the crystallization exotherms of the PBT in the (PBT/GF)/PC and (PBT/GF)/IM/PC shifted towards lower temperatures, revealing that, under the influence of the PC, the PBT crystallization needs a higher degree of supercooling. These results indicate that, with the occurrence of PBT-PC transesterification, some of the PBT segments were substituted by the PC segments, which decreased the regularity of the PBT chains and, in turn, weakened the crystallization ability of the PBT. As a result, the crystallization rate of the PBT was slowed down and crystallites with low perfection were formed.
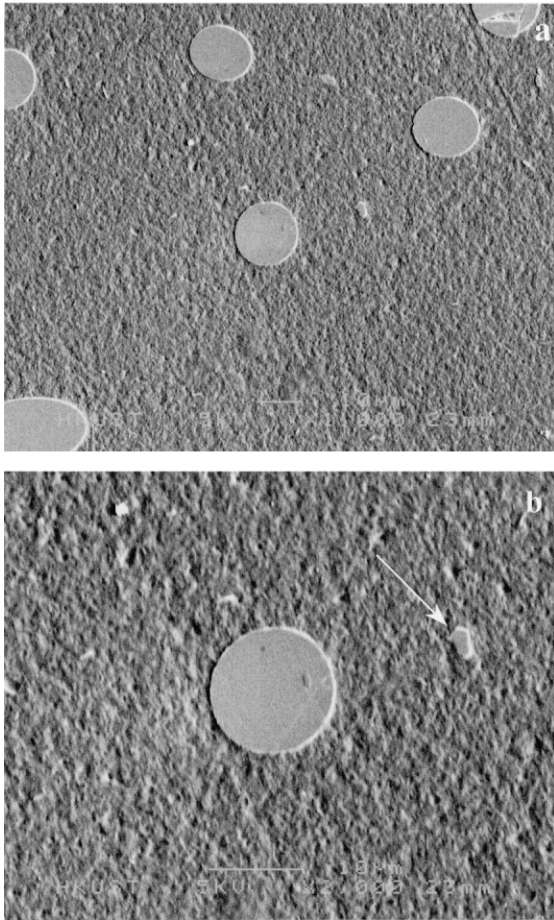
Fig. 10. SEM micrographs of the KOH etched surface of the (PBT/GF)/IM/PC: (a) ×1000; (b) ×2000.

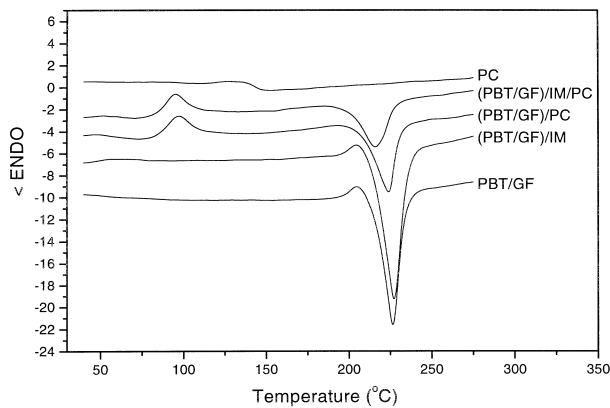Fig. 11. DSC thermograms of the first heating run.

Fig. 12. DSC thermograms of the cooling run.
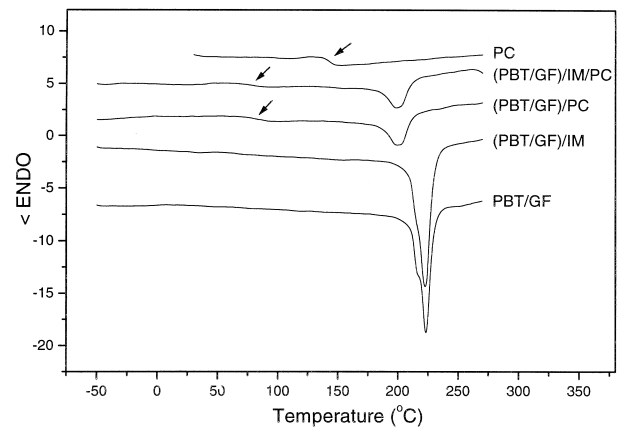
Fig. 13. DSC thermograms of the second heating run.

Table 2
DSC crystallization and melting data

Sample	T_g (°C)		T_m (°C)		T_c (°C)	T_c (°C)	X_c (%)
	First run	Second run	First run	Second run	Cooling	Heating (first run)	
PBT/GF			226.45	223.28	212.36	None	44.92
PC	142.82	143.36				None	
(PBT/GF)/ IM			227.17	222.68	211.22	None	44.77
(PBT/GF)/ PC		79.61	223.96	201.18	187.42	97.2	42.91
(PBT/GF)/ IM/PC		80.04	216.10	199.04	185.99	95.22	39.61

The thermograms of the second heating scan give further evidence about the miscibility between PBT and PC. As can be seen in Fig. 13 and Table 2, the glass transition of the PC phase in the (PBT/GF)/PC and (PBT/GF)/IM/PC shifted to lower temperatures. The crystallinity of the PBT in the (PBT/GF)/PC and (PBT/GF)/IM/PC composites was lower than that in the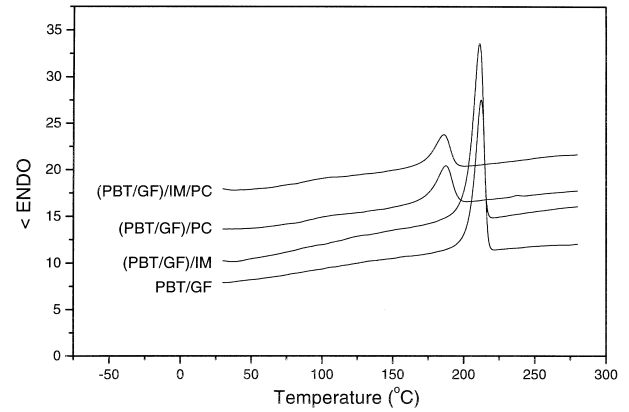 (PBT/GF). All the phenomena suggest that PC has a relatively high miscibility with the PBT in the current composite systems.

3.3.2. PBT/IM

We have suggested that the IM domains are encapsulated in the PBT phase based on the AFM and SEM observations. However, it was found, based on the results in Figs. 11–13 and Table 2, that the PBT in the

(PBT/GF) and (PBT/GF)/IM has similar melting and crystallization behavior. In other words, addition of the IM has little effect on the thermal behavior of PBT. This finding implies that IM is immiscible with the PBT and there is no specific strong interaction between the two components.

The IM used in the current work is an ethylene-co-glycidyl methacrylate copolymer (E-GMA). Studies [22–25] have demonstrated that the epoxide groups in the E-GMA copolymers can react with the terminal carboxylic acid and/or hydroxyl groups of PET, PBT and PC via nucleophilic substitution under appropriate conditions. On the other hand, it is also pointed out in [25] that the epoxide groups can polymerize via ring-opening reaction in the presence of initiators and forms a cross-linked structure. The rate of these reactions can be altered considerably by the presence of catalysts [25]. The residual catalyst from the PBT synthesis, possibly metal ions, and other contaminants from the polymerization or processing may influence the reactions.

Based on the above experimental evidence, we propose that the dominant reaction during the melt blending of the IM and the (PBT/GF) seems the ring-opening homo-polymerization of the epoxide groups. A slightly cross-linked structure formed in the IM phase. Thus, during the first step of the sequential compounding, the IM phase dispersed extensively in the PBT phase. The domain size and shape were solidified by partial cross-linking. In the second step of the sequential compounding, the IM had no functional group to react with the PC; thus, there was no driving force to promote the IM domains to migrate from the PBT phase to the PC phase. By comparing the thermograms of the (PBT/GF)/PC and (PBT/GF)/IM/PC in Fig. 13, it can be found that the glass transition of the PC was unaffected by the presence of the IM, confirming that there was no specific interaction or chemical bonding between the PC and the IM.
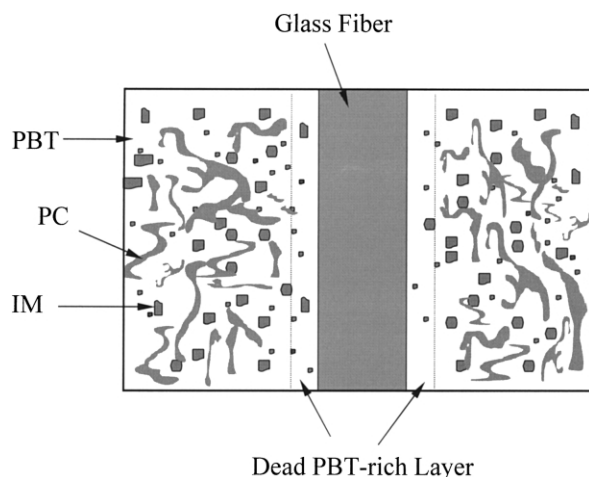
In summary, the designed (PBT/GF)/IM/PC composite has a morphology shown schematically in Fig. 14. The glass fiber of the composite is surrounded by a dead layer of PBT-rich resin. In the matrix, because of the high miscibility of the PBT and PC, the two components form a fine, interconnected phase structure with the PBT domain thickness of about 1 μm and the PC domain thickness of less than 0.5 μm. The IM particles are mostly located in the PBT phase and have a particle size varying between 0.5 to 1 μm.

4. Conclusions

Glass fiber reinforced PBT/PC/IM composites with controlled morphology were designed and produced via sequential blending. The morphology of the composites was characterized by means of AFM, SEM and thermal analysis. The results indicate that the glass fibers were surrounded by a sheath of PBT-rich resin. The thickness of this sheath varied with the composite composition. It was about 0.2 μm in the (PBT/GF) and the (PBT/GF)/PC, 0.5 μm in the (PBT/GF)/IM and 5 μm in the (PBT/GF)/PC/IM composites.

Regarding the matrix microstructures of the (PBT/GF)/PC/IM composite, though the PBT was immiscible with the IM, the elastomer domains were still located in the PBT phase because of the sequential blending technique used. It was proposed that, when the (PBT/GF) was mixed with the IM in the first step of the sequential blending process, the epoxide groups in the IM might have undergone the homo-polymerization through ring-opening mechanism rather than to react with the terminal carboxylic acid and/or hydroxyl groups of the PBT. Consequently, a slightly cross-linked structure formed in the IM phase. Due to its low reactivity, the cross-linked IM particles would stay in the PBT phase during the second step of the sequential blending with the PC. The particle size of the IM domains varied between 0.5 and 1 μm.

The PBT-PC transesterification enhanced the miscibility of the two components, leading to a very fine interconnected microstructure, where the PBT domain thickness is about 1 μm and the PC less than 0.5 μm. The transesterification violated, to a certain extent, the regularity of the PBT chains, which decreased the crystallization ability of the PBT and resulted in a declined crystallization rate and the formation of imperfect crystallites.

Fig. 14. Schematic representation of the phase structure of the (PBT/GF)/IM/PC composites.

Acknowledgements

References

[1] Kurauchi T, Ohta T. Energy absorption in blends of polycarbonate with ABS and SAN. J Mater Sci 1984;19:1699–709.

[2] Koo K, Inoue T, Miyasaka K. Toughened plastics consisting of brittle plastics and ductile matrix. Polym Eng Sci 1985;25:741–6.

[3] Sue H, Yee AF. Toughening mechanisms in a multi-phase alloy of nylon 6,6/polyphenylene oxide. J Mater Sci 1989;24:1447–57.

[4] Wu JS, Mai Y-W. Ductile fracture and toughening mechanisms in polymers. Materials Forum 1995;19:181–99.

[5] Okamoto M, Shinoda Y, Kojima T, Inoue T. Toughening mechanism in a ternary polymer alloy: PBT/PC/rubber system. Polymer 1993;34:4868–73.

[6] Lu ML, Chang FC. Fracture toughness of PC/PBT blend based on J-integral methods. J Appl Polym Sci 1995;56:1065–75.

[7] Hopfe I, Pompe G, Eichhorn KJ. Ordered structures and progressive transesterification in PC/PBT meltblends studied by FTi.r. spectroscopy combined with d.s.c. and n.m.r.. Polymer 1997;38:2321–7.

[8] Mishra SP, Venkidusamy P. Structural and thermal behavior of PC/PBT blends. J Appl Polym Sci 1995;58:2229–34.

[9] Montaudo G, Puglisi C, Samperi F. Mechanisms of exchange in PBT/PC and PET/PC blends. Composition of the copolymer formed in the melt mixing process. Macromolecules 1998;31:650–61.

[10] Wu JS, Mai Y-W, Cotterell B. Fracture toughness and fracture mechanisms of PBT/PC/IM blends; Part 1. Fracture properties. J Mater Sci 1993;28:3373–84.

[11] Wu JS, Mai Y-W. Fracture toughness and fracture mechanisms of PBT/PC/IM blends, Part II toughening mechanisms. J Mater Sci 1993;28:6167–77.

[12] Wu JS, Mai Y-W, Yee AF. Fracture toughness and fracture mechanics of polybutylene-terephthalate/polycarbonate/impact modifier blends, Part III. Fracture toughness and mechanics of PBT/PC blends without impact modifiers. J Mater Sci 1994;29:4510–22.

[13] Wu JS, Yu D-M, Mai Y-W, Yee AF. Fracture toughness and fracture mechanisms of PBT/PC/IM blends, Part IV Impact toughness and failure mechanisms of PBT/PC blends without impact modifier. J Mater Sci 2000;35:1–9.

[14] Wu JS, et al., Fracture toughness and fracture mechanisms of PBT/PC/IM blends, Part V. Interface optimization by adding in-situ formed copolymers, J. Mater. Sci. (submitted).

[15] Wang K, Wu JS. Mechanical properties and fracture mechanisms of fiber reinforced PBT/PC/elastomer blends. Key Eng Mater 2000;177-180:363–8.

[16] Wang K, Wu JS. Microstructure and fracture behavior of glass fiber reinforced PBT/PC/elastomer blends II. Fracture behavior and toughening mechanisms. J Polym Sci, Polym Physics (submitted).

[17] Devaux J, Godard P, Mercier JP. Bisphenol-A polycarbonate-poly(buthylene terephthalate) transerterification-1. Theoretical study of the structure and of the degree of randomness in four-component copolycondensates. J Polym Sci, Polym Phys Ed 1982;20:1875–80.

[18] Hobbs SY, Groshans VL, Dekker MEJ, Shultz AR. Partial miscibility of poly(butylene terephthalate)/BPA polycarbonate melt blends. Polym Bull 1987;17:335–9.

[19] Hobbs SY, Watkins VH, Brendler JT. Diffusion bonding between BPA polycarbonate and poly(butylene terephthalate). Polymer 1990;31:1663–8.

[20] van der Velden G, Kolfschoten-Smitsman G, Veermans A. ^{13}C CP/MAS NMR, draft and ATR/FTIR study of a solid poly-carbonate-poly(butylene terephthalate) blend: evidence for trans-esterification. Polym Comm 1989;28:169–71.

[21] Pompe G, Häußler L. Investigation of transesterification in PC/PBT melt blends and the proof of immiscibility of PC and PBT at completely suppressed transesterification. J Polym Sci, Polym Phys Ed 1997;35:2161–8.

[22] Tsai CH, Chang FC. Polymer blends of PBT and PP compatibilized by ethylene-co-glycidyl methacrylate copolymers. J Appl Polym Sci 1996;61:321–32.

[23] Kudva RA, Keskkula H, Paul DR. Compatibilization of nylon 6/ABS blends using glycidyl methacrylate/methyl methacrylate copolymers. Polymer 1998;39:2447–60.

[24] Hale W, Kekkula H, Paul DR. Compatibilization of PBT/ABS blends by methyl methylacrylate-glycidyl methylacrylate-ethyl acrylate terpolymers. Polymer 1999;40:365–77.

[25] Stewart ME, George SE, Miller RL, Paul DR. Effect of catalyst on the reactive processing of polyesters with epoxy-functional polymers. Polym Eng Sci 1993;33:675–85.